Revista Brasileira de Geografia Física v.19, n.02. (2026) 814-830.

Revista Brasileira de Geografia Física

ISSN:1984-2295

Homepage: https://periodicos.ufpe.br/revistas/rbgfe

Air Pollution Assessment by Landsat Aerosol-Level Mapping in the Macrometropolitan Region of São Paulo, Brazil

Isabella Borges[1] ,Julia Lanci Rodrigues[2], Nathalia Banharoto Dutra da Silva[1], Beatrice Mika Saito[3], Vitor Vieira Vasconcelos[4]

[1] Environmental Analyst – New Fields, [2] Product Analyst – Itaú Unibanco, [3] M.Sc. candidate – Post-Graduate Program of Environmental Science and Technology, Federal University of ABC. GIS Analyst – Companhia de Saneamento Básico do Estado de São Paulo - Sabesp. [4] Professor. Federal University of ABC.

Article received on 02/10/2025 and accepted on 02/21/2026

A B S T R A C T

The accelerated process of industrialization and urbanization in the Metropolitan Region of São Paulo (MRSP) and the Metropolitan Region of Baixada Santista (MRBS), associated with the exploitation of natural resources and patterns of territorial occupation, resulted in quality-of-life degradation, including urban air pollution. The objective of this study was to present an observational analysis of the temporal variability of aerosol optical depth, based on remote sensing products, for two specific dates. Landsat 8 and 9 aerosol-quality layers were used to produce aerosol level maps in the MRSP and Baixada Santista, combining them with monitoring data from the Environmental Company of the State of São Paulo (CETESB). The hypothesis explored was that there is a relationship between the concentration of particulate matter and its emission sources. Notably, AOD level data derived from Landsat are useful for assessing near-surface urban atmospheric aerosols and mapping areas influenced by aerosol pollution. Furthermore, it is advisable to combine these data with continuous ground-based air pollution monitoring in the MRSP and Baixada Santista.

Keywords: Particulate matter, Air quality monitoring, Remote sensing, Traffic and industrial emissions.

Avaliação da poluição atmosférica por meio do mapeamento níveis de aerossóis por satélites Landsat na macro-região metropolitana de São Paulo, Brasil.

R E S U M O

O acelerado processo de industrialização e urbanização da Região Metropolitana de São Paulo (MRSP) e da Baixada Santista (RMBS), associado ao padrão de exploração dos recursos naturais e ocupação territorial, resultou na degradação da qualidade de vida das populações, a exemplo da poluição do ar urbano. O objetivo deste estudo foi apresentar uma análise observacional da variabilidade temporal da profundidade óptica do aerossol, com base nos produtos de sensoriamento remoto, para duas datas específicas. Para isso, utilizaram-se dados de da camada de qualidade de aerossol dos satélites Landsat 8 e 9 a fim de elaborar mapas de nível de aerosol na MRSP e Baixada Santista e conjugá-los com dados de monitoramento da Companhia Ambiental do Estado de São Paulo (CETESB). A hipótese explorada foi que há uma relação entre a concentração de material particulado e as suas fontes de emissão. Dentre os resultados, destaca-se que os dados de AOD baseados no Landsat são úteis para a avaliação de aerossóis atmosféricos urbanos ao nível do solo e mapeamento de áreas de influência da poluição por aerossóis. Ainda, aconselha-se a conjugação desses dados com o monitoramento contínuo da poluição do ar na MRSP e Baixada Santista.

Palavras-chave: Material particulado, Monitoramento da qualidade do ar, Sensoriamento Remoto, Emissões industriais e de tráfego.

Introduction

One of the biggest threats to global environmental health is air pollution, which has a significant impact on megacities that are experiencing rapid industrial and urban growth. In response to strong epidemiological evidence that there is no safe threshold of exposure, the 2021 update of the World Health Organization (WHO) Global Air Quality Guidelines halved the recommended annual mean limits for fine particulate matter ($PM_{2.5}$) to 5 µg/m³ and lowered PM_{10} limits to 15 µg/m³ (Hoffmann et al., 2021; Tang & Kumar, 2022). Approximately 6.7 million people die each year due to air pollution, including particulate matter (PM) air pollution, and it is estimated that approximately 99% of the world's population lives in places where air quality does not meet WHO guidelines as of 2023 (WHO, 2023).

Of the total number of CETESB monitoring stations in the State of São Paulo, 92% showed, in 2021, pollutant concentrations exceeding the annual averages recommended by the WHO (CETESB, 2022). The vehicular fleet is the main source of air pollution in the Metropolitan Region of São Paulo (Gavidia-Calderón et al., 2024). In the MRSP, the consequences of air pollution are evident across multiple health outcomes, such as cardiopulmonary effects, low birth weight, increased hospital utilization, the incidence of several types of cancer, and mortality among children and the elderly, which mainly affect the most economically vulnerable segments of the population (Bravo et al., 2016; Gouveia et al., 2017; Singer et al., 2023).

Given the magnitude of the association between air pollution and the health of São Paulo residents, it is estimated that the capital São Paulo could save US$15.1 billion annually if the city met the $PM_{2.5}$ standards recommended by the WHO (Abe & Miraglia, 2016). Meeting WHO standards would also prevent an estimated 113 and 24 annual deaths from lung cancer and chronic obstructive pulmonary disease, respectively, as well as 258 and 163 hospitalizations caused by respiratory and cardiovascular diseases, respectively, due to PM2.5 exposure (Wikuats et al., 2023).

Air quality measurement by fixed monitoring stations allows real-time and continuous, long-term assessment of compliance with environmental standards and regulations. However, this monitoring strategy has limited geographic coverage; therefore, it is limited in estimating pollutant levels in areas far from the stations.

Aerosols are stable hybrid particles composed of solid and/or liquid components that are dispersed in the atmosphere (Mansour et al., 2024). Primary aerosols and precursor gases—such as sulfur dioxide (SO_2), nitrogen oxides (NO_x), carbon monoxide (CO), and particulate matter (PM), including resuspended dust—are present in polluted atmospheres (Meo et al., 2024).

Aerosol particles dispersed in the atmosphere interact, directly or indirectly, with solar and infrared radiation incident on Earth. Direct interaction consists of the absorption and scattering of solar radiation. Indirect interaction, on the other hand, consists of modification of cloud microphysical processes (e.g., cloud condensation nuclei activity), which can affect cloud formation and radiative properties. Aerosol particles, when interacting with solar or infrared radiation, can absorb or scatter radiation, thereby attenuating the direct radiative beam (Li et al., 2022).

Accordingly, aerosol optical depth (AOD) is related to the wavelength of the incident radiation. The relevance of AOD is directly related to the concentration of particles throughout the vertical column of the atmosphere (Zhu et al., 2024). In other words, AOD is the exponential attenuation factor of the direct solar radiation as it passes through the atmosphere, reflecting interactions with aerosols and the wavelength-dependent information on the aerosol size distribution (Liu et al., 2023). This metric is used to characterize the degree of atmospheric turbidity, estimate the aerosol content in the atmosphere, and assess the degree of atmospheric pollution (Zhu et al., 2024).

Atmospheric correction is applied to remove interference from the atmosphere (such as aerosols and water vapor) in remote sensing images and to allow estimation of surface reflectance by correcting top-of-atmosphere (TOA) reflectance (Nazeer et al., 2021). The difference between top-of-atmosphere reflectance and surface reflectance can be interpreted as part of the atmospheric signal, and simulation studies show that this TOA–surface reflectance difference varies with aerosol optical depth and aerosol single-scattering albedo (Qi et al., 2022). Soleimany et al. (2022) proposed using multiple regression models to compare this band difference with monitoring station data and to generate integrated maps of ambient particulate matter concentration.

The MODIS satellite has been used in several regional-scale air pollution mapping studies at 250 m resolution for selected bands (e.g., Qayyum et al., 2022). Previous studies found a relationship between air pollution, AOD, and distinct periods of vehicle traffic intensity in São Paulo State (Rudke et al., 2023) and in the Metropolitan Region of São Paulo (Pérez-Martínez et al., 2022), using satellite and ground-based monitoring data. However, the coarse spatial resolution of these satellites cannot capture intra-urban microclimates and their localized emission plumes (Qin et al., 2022).

For higher-resolution mapping, several studies have applied this approach with Landsat images (Soleimany et al., 2022; Sheng et al., 2023). However, one of the challenges of working with higher-resolution images is dealing with image noise arising from local clouds and surface characteristics of land-cover features.

Earlier studies have used simpler atmospheric correction models, such as dark pixel subtraction (Shah et al., 2025). Subsequently, Vermote et al. (2016) developed more advanced atmospheric correction models, including ultra-blue (aerosol) and shortwave-infrared (water vapor) bands available on MODIS, Landsat-8, and Sentinel-2. These models enable improved estimation of spatial variation in atmospheric attenuation across each satellite scene (Groeneveld et al., 2024), and provide an additional band containing estimates of atmospheric aerosol optical depth. These products open up new opportunities for mapping air pollution using satellite imagery.

Despite recent advances in aerosol mapping using remote sensing, particularly with the increasing availability of high-resolution satellite imagery (Ranjan et al., 2021), several limitations and uncertainties remain. The main challenge is the disentanglement of atmospheric turbidity caused by aerosols from that associated with water vapor, which has been noted for the LaSRC atmospheric correction model (Vermote et al., 2016; Jin et al., 2022) currently used for Landsat and also adapted for Sentinel satellites.

Another well-documented limitation of the LaSRC algorithm is estimating aerosol loading over surfaces with high reflectance (e.g., bright materials) (Groeneveld et al., 2024; Sun et al., 2016; Vermote et al., 2016), which is common for several surfaces in urban areas, central to this study. Furthermore, a substantial share of aerosols transported by winds originates from wind erosion (especially from deserts), biomass burning (wildfire and agriculture), sea-salt emissions, and volcanic sulfur compounds (Putman, 2014; Hamilton et al., 2022), and it becomes a challenge to separate these global fluxes from local sources of air pollution in the urban environment, especially in cities frequently affected by these regional fluxes.

The objective of this study is to evaluate the spatial coherence between ground-level particulate matter concentrations across the Macrometropolitan Region of São Paulo and high-resolution (30 m) aerosol optical depth (AOD) retrievals obtained from the Landsat 8 and 9 Land Surface Reflectance Code (LaSRC) algorithm. Moving beyond general regional evaluations, this study hypothesizes that, although localized anthropogenic emission hotspots can be identified using high-resolution satellite imagery, the underlying physical algorithms show substantial uncertainties over highly reflective urban surfaces.

With this aim, this study examines the spatial coherence between aerosol plumes and localized anthropogenic emission sources, such as mining sites, high-traffic corridors, and industrial complexes, by comparing satellite-derived AOD with ground-based monitoring data from the Aerosol Robotic Network (AERONET) (NASA, 2023) and the QUALAR system from São Paulo State Environmental Company (CETESB, 2022). Furthermore, this study explicitly evaluates the limitations of AOD retrievals over complex, heterogeneous urban and coastal surfaces, providing insights for complementing sparse ground-based monitoring networks with remote sensing data.

Materials and methods

Data collection

Landsat-8 and 9 images

Landsat 8 and 9 satellite images were selected from the catalog provided by USGS *EarthExplorer*[1](USGS, 2023). The search for images covered the entire period available for each satellite from April 2013 to June 2023 for Landsat 8, and September 2021 to June 2023 for Landsat 9, encompassing the pre- and post-COVID-19 pandemic periods. Image selection criteria were: (i) image quality; (ii) the absence of clouds; and (iii) minimal or no noise.

Images that had undergone orthorectification and atmospheric correction (*Landsat Collection 2, Level 2*) were selected. For the MRSP and Baixada Santista study areas, two cloud-free images were identified to avoid bias in the aerosol identification algorithm:

1. Image 1, ID LC08_L2SP_219076_20190817_20200827_02_T1, dated August 17, 2019.
2. Image 2, LC09_L2SP_219076_20220529_20230415_02_T1, dated May 29, 2022.

For this study, only the bands with the estimated aerosol intensity (SR_QA_AEROSOL bit-packed aerosol QA layer, generated by the atmospheric correction algorithm) and the water surface mask from both images were used. The aerosol intensity estimation layers provided by the Sentinel-2 satellite for the same dates were analyzed (see Supplementary Material), but the Sentinel-2 results were shown to be strongly affected by humidity near water bodies; therefore, they were excluded from the analysis.

[1] https://earthexplorer.usgs.gov/ , accessed November 14, 2023.

Air quality values and meteorological data

Gavidia-Calderón et al. (2024) suggested the combined use of satellite data with the CETESB air quality network to improve spatial assessment of air quality in the Metropolitan Region of São Paulo. The DataGeo (2023) catalog of Monitoring Stations for Inhalable Particles (PM_{10}) in the State of São Paulo was used to select the stations located within the chosen satellite images. To select reference air quality and climate values for the image dates, the CETESB Air Quality Information System (QUALAR) was used. The parameters chosen were PM_{10} (inhalable particles) and, when available, temperature, relative humidity, and wind speed.

Additionally, data on daily average AOD for the study dates were collected from NASA (2023) Aerosol Robotic Network (AERONET). There are two AERONET stations within the study area, both located in the city of São Paulo: São Paulo (Butantã) and EACH-USP (Ermelino Matarazzo). Only Level 2 AERONET data were used, which are already subjected to corrections to compensate for atmospheric and instrumental effects, such as calibration, scattering, and atmospheric absorption.

Figure **1** shows the location of CETESB and AERONET stations in the State of São Paulo.

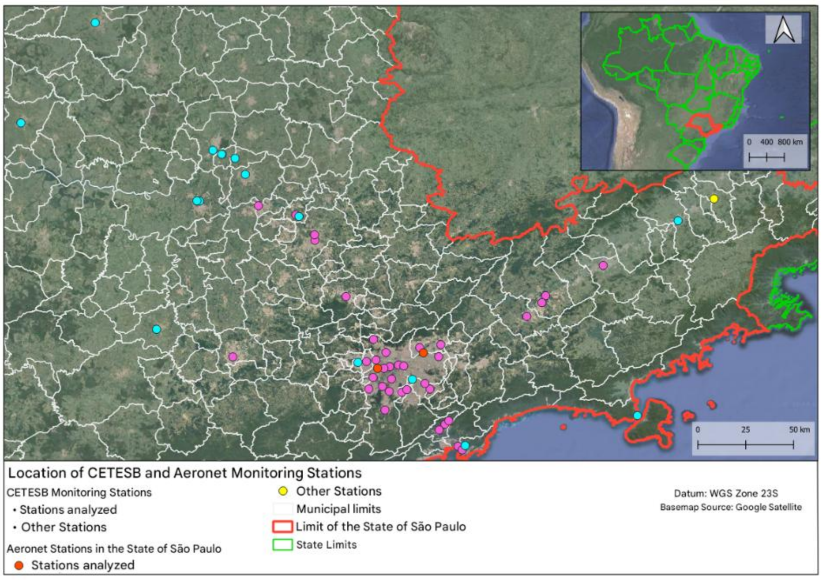

Figure 1. Location of CETESB and AERONET monitoring stations.

Manipulation of satellite images

The aerosol intensity band generated by the atmospheric correction algorithm has values from 0 to 255, but these values have no physical meaning. To analyze the images, the pixel values were reclassified into three groups: low aerosol level (binary 01, values 0-100), medium aerosol level (binary 10, values 101-190), and high aerosol level (binary 11, values >190), as described in the documentation for the Landsat-8 atmospheric correction model (USGS, 2020). This reclassification is necessary because the pixel value encodes other characteristics of the data, such as the level of uncertainty, presence of water and clouds, and the sampling and interpolation procedures used by the atmospheric correction algorithm. The USGS (2020) documentation does not provide a physical reference of what is considered a low, medium, or high level of aerosol loading.

Analysis of the relationship between anthropogenic activity and aerosols

An observational assessment was carried out to examine the relationship between AOD and anthropogenic activity at specific points in the study area. Furthermore, the influence of the type of activity present in these places and its possible impacts on air quality via increased aerosol concentrations were discussed.

For the observational evaluation, the study areas were divided according to their dominant pollutant source. Thus, the four groups were: (i) industrial areas; (ii) areas of high automobile circulation; (iii) mining areas; and (iv) water-influenced areas. Figure **2** shows the location of the analyzed areas according to these four source categories.

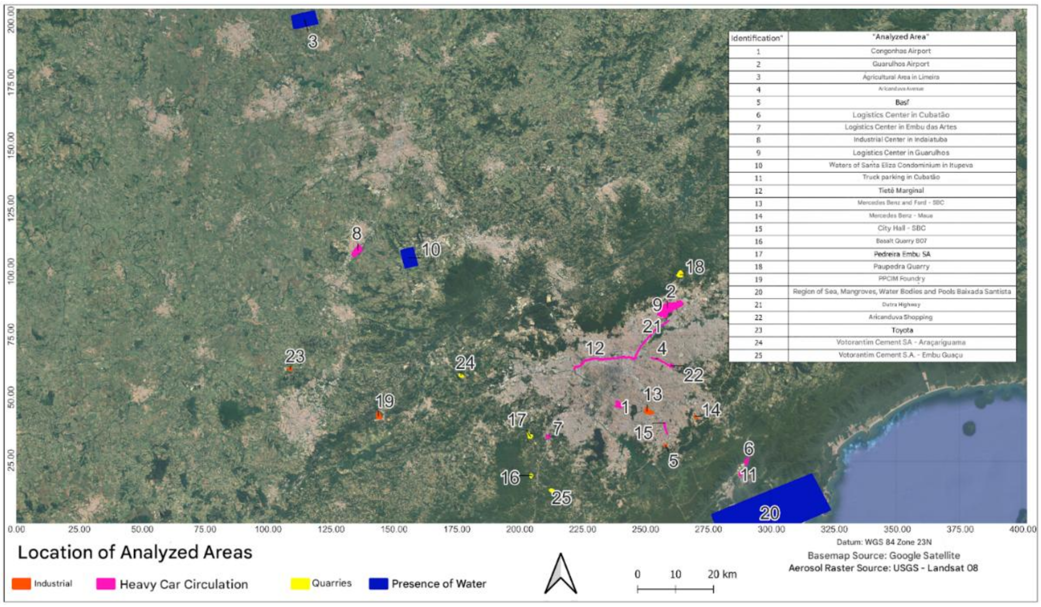

Figure 2. Location of the areas analyzed according to group classification.

Results and discussion

Temporal variability of AOD among satellite images

When comparing the satellite images from August 17, 2019, and May 29, 2022, as shown in **Figure 3**, a greater spatial extent of aerosol dispersion over the MRSP and Baixada Santista is observed for 2022. The areas mapped in pink (medium aerosol levels) have expanded. The increase in atmospheric aerosol in the 2022 image suggests higher emissions and/or meteorological conditions favoring aerosol accumulation, mainly to the east of the MRSP. It is important to keep in mind that August 17, 2019 was a Saturday, and May 29, 2022 was a Sunday, days with typically lower traffic, and therefore, weekday vehicle-related aerosol emissions may be higher, all else equal.

When analyzing the data from CETESB monitoring stations with measurements on both dates, it is noted that mean PM_{10} concentrations were higher on August 17, 2019, than on May 29, 2022 (average of 49.6 μg/m^3 and 42.3 μg/m^3, respectively), and that the average temperature in 2019 (28.3 ºC) was higher than in 2022 (15.8 ºC). On the other hand, the average relative humidity in 2019 (32.4%) was lower than that in 2022 (56.7%), and the average wind speed was lower in 2019 (1.5 m/s) than in 2022 (2.0 m/s).

One possible interpretation is that the increase in wind speed between 2019 and 2022 dates caused greater horizontal dispersion of aerosols, thereby decreasing particulate matter concentrations. Han et al. (2021) observed a similar effect in Beijing, where particulate matter and aerosol concentrations were higher under wind speeds below 2 m/s. Leirião et al. (2023) found that wind speed and PM_{10} were associated with cardiorespiratory mortality among the elderly in the city of São Paulo, possibly linked to pollutant dispersal.

However, another explanation for the increase in aerosol patches in 2022 could be the algorithmic misclassification due to the higher water vapor content (i.e., higher relative humidity). This is a complex relationship because, despite the turbidity caused by water vapor, water molecules in the air also promote the aggregation of dust particles into water droplets, which in turn increases light scattering capacity (Xu et al., 2005; Rodriguez-Loya et al., 2023). The hygroscopic growth of hydrophilic aerosol particles suspended over the metropolitan area may have been facilitated by the much higher ambient relative humidity recorded during the satellite overpass in May 2022 (56.7%) compared to the drier conditions of August 2019 (32.4%), which consequently alters the aerosol optical scattering properties. The effective volumetric radius of these ambient particles increases as they absorb atmospheric moisture, leading to a significant increase in their optical scattering cross-section. On the other hand, in drier periods, there may be a greater amount of dust lifted from non-cohesive sediments by wind forcing (Jebali et al., 2021). Leirião et al. (2023) also found that air humidity and seasonality, when analyzed together with PM_{10} and other pollutants, were associated with cardiorespiratory mortality among the elderly in the city of São Paulo.

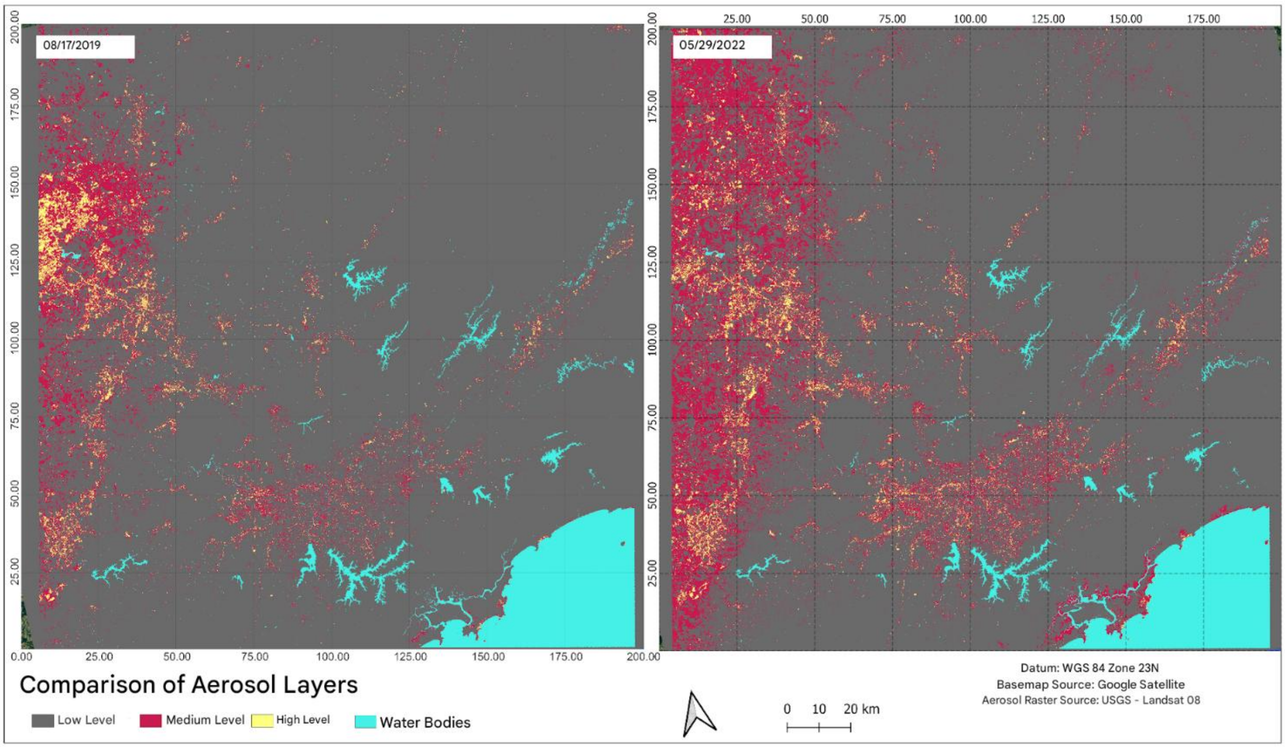

Figure 3: Temporal comparison of AOD between 2019 (left) and 2022 (right).

Comparison of CETESB, AERONET and AOD results

Table **1** summarizes the PM_{10} results according to the aerosol level assigned to each station. The results for each monitoring station are presented in the Supplementary Material.

Table **2** summarizes the daily mean AOD on 17 August 2019 and 29 May 2022, based on historical AERONET data for the monitoring sites present in the study area. AOD is a unitless measure of column-integrated aerosol loading; higher values indicate greater aerosol abundance.

Table 1. Mean and standard deviation of PM_{10} of the stations for each aerosol class. Source: CETESB, 2023.

		08/17/2019	
Classification by layer aerosol	**Number of stations**	**PM_{10} average ($\mu g/m^3$)**	**σ**
Low aerosol level	19	45.95	18.42
Average aerosol level	5	63.60	18.43
High aerosol level	0	-	-
		05/29/2022	
Low aerosol level	12	47.77	28.34
Average aerosol level	7	36.00	5.29
High aerosol level	3	35.33	4.92

Note: σ – standard deviation

Table 2. Average AOD of AERONET monitoring stations. Source: NASA, 2023.

Date	Number of stations with data	Mean AOD at 500 nm	Standard deviation
08/17/2019	2	0.1032	0.0028
05/29/2022	2	0.1211	0.0031

Obs: AOD measurement wavelength: 500 nm

From the analysis of **Tables 1 and 2**, three observations can be made:

I. There is no spatial coincidence between the spots with the highest aerosol concentration in the satellite images and the location of CETESB monitoring stations, which raises questions about whether the current siting of these stations is adequate for monitoring and risk assessment.

II. The PM_{10} values at CETESB stations were higher in areas with lower aerosol levels. One hypothesis is a spatial-scale mismatch, comparing the local, point-based measurement at each station with the satellite-derived aerosol map on 30 m Landsat pixels.

III. Finally, AERONET indicates a higher mean AOD in 2022 than in 2019. However, caution is needed when comparing the observational analysis of the images and the CETESB data with the AOD data from AERONET, mainly because the latter has fewer monitoring stations, making it insufficient to diagnose AOD levels across the entire study area. Furthermore, particulate matter is measured close to the Earth's surface (CETESB, 2023), while AOD represents aerosol optical effects integrated over the entire atmospheric column (Bilal et al., 2022).

Analysis of the relationship between anthropogenic activity and aerosols

The following sections present and analyze the aerosol-intensity maps for the selected critical areas. The most representative sites of each aerosol source typology are presented and discussed, and maps for the remaining areas shown in Figure 2 are provided in the Supplementary Material.

<u>Industrial areas</u>

In industrial areas, aerosols may originate from pollutant emissions associated with the production process itself (released into the atmosphere through stacks) or from high vehicle traffic and the operation of combustion engines on industrial premises. Figure **4** illustrates the first group, as it includes production processes that transform raw materials and generate particles emitted into the air. By contrast, Figure **5** illustrates the second group and, coincidentally, corresponds to automobile assembly plants. Although these facilities do not involve substantial material transformation, the operations entail intense circulation of combustion-powered vehicles.

The only CETESB monitoring station within the analyzed industrial areas is the São Bernardo-Paulicéia station, as shown in **Figure 5**. Regarding the PM_{10} concentrations for the study dates, 37.0 µg/m³ was recorded in 2019 and 31.0 µg/m³ in 2022. Regarding wind speed, 1.7 m/s was recorded in 2019 and 2 m/s in 2022. Temperature and relative humidity were not available for these dates at the Paulicéia Station. Although differences in AOD are not visually pronounced between the two years (Figure 5), the CETESB PM_{10} record indicates lower particulate levels in 2022, which may reflect changes in local emissions, including the deactivation of the Ford São Bernardo automobile assembly plant.

Figure 4. BASF in São Bernardo do Campo - SP.

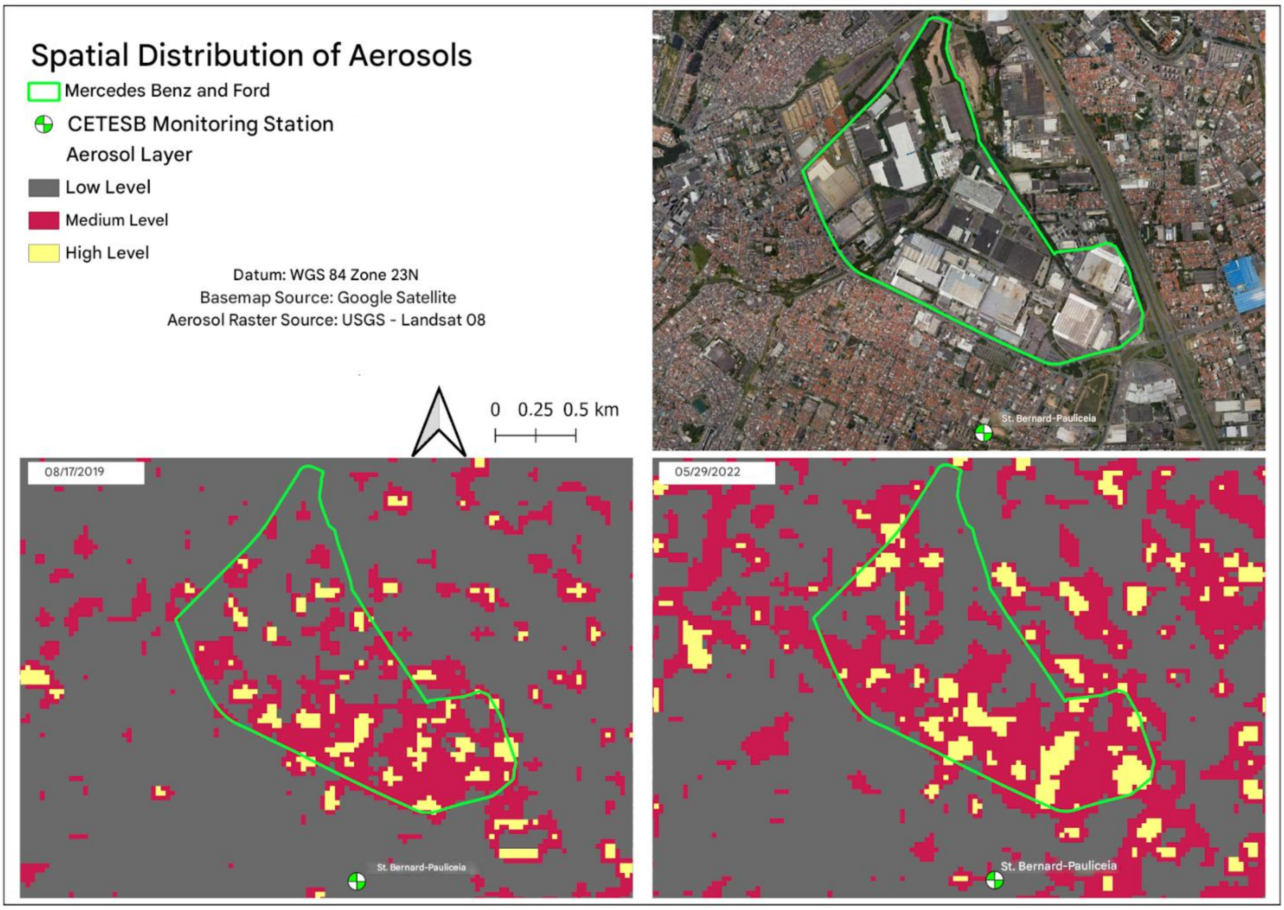

Figure 5. Mercedes-Benz and Ford in São Bernardo do Campo - SP.

An important aspect in the analysis of industrial plants is that many areas classified as high aerosol level, especially the roofs of warehouses, have high reflectance (e.g., white surfaces), which corresponds to a known difficulty in estimating aerosol using Landsat-8 atmospheric correction algorithms (Groeneveld et al., 2024; Sun et al., 2016; Vermote et al., 2016). However, mapped aerosol patches also extend to vehicle yards and factory access areas, which are typically darker. In addition, several other bright surfaces around these facilities were not classified as high aerosol levels, underscoring the spatial specificity of the mapped patterns. Therefore, it cannot be stated that the aerosol-mapping layer systematically favored buildings or other land-cover types with higher reflectance.

Areas with heavy car traffic

The map in **Figure 6 (Guarulhos Airport)** shows little difference in AOD between the two studied years. The highest aerosol levels appear in logistics areas adjacent to the airport, where vehicle traffic is high, rather than on the runway. At the nearest CETESB station (Guarulhos-Paço Municipal), PM_{10} was 42.0 $\mu g/m^3$ in 2019 and 34.0 $\mu g/m^3$ in 2022.

Figure 7 illustrates the case of large avenues or highways. Across all sites of this type (see Supplementary Material), the wider spatial extent of aerosol in 2022 is noticeable. For the sites with CETESB coverage, **Figure 7** shows that the Marginal Tietê-Ponte Remédios station recorded PM_{10} concentrations of 54.0 $\mu g/m^3$ in 2019 and 41.0 $\mu g/m^3$ in 2022 (see **Table 3** for details). These values suggest that, although PM_{10} was lower on 29 May 2022, meteorological conditions–colder temperatures, higher relative humidity, and stronger winds than on 17 August 2019–may have contributed to enhanced aerosol dispersion.

Table 3. Historical data of the Tietê Marginal Station - Ponte Remédios. Source: CETESB, 2023.

	PM_{10} ($\mu g/m^3$)	RH (%)	TEMP (ºC)	VV (m/s)
08/17/2019	54.0	28.0	26.9	1.7
05/29/2022	41.0	60.0	14.0	2.7

Finally, **Figure 8** shows an example of parking lots in logistics centers. Again, an intensification in the presence of pink (medium aerosol level) and yellow (high level) pixels is observed in 2022. A similar pattern is observed in shopping-center parking lots.

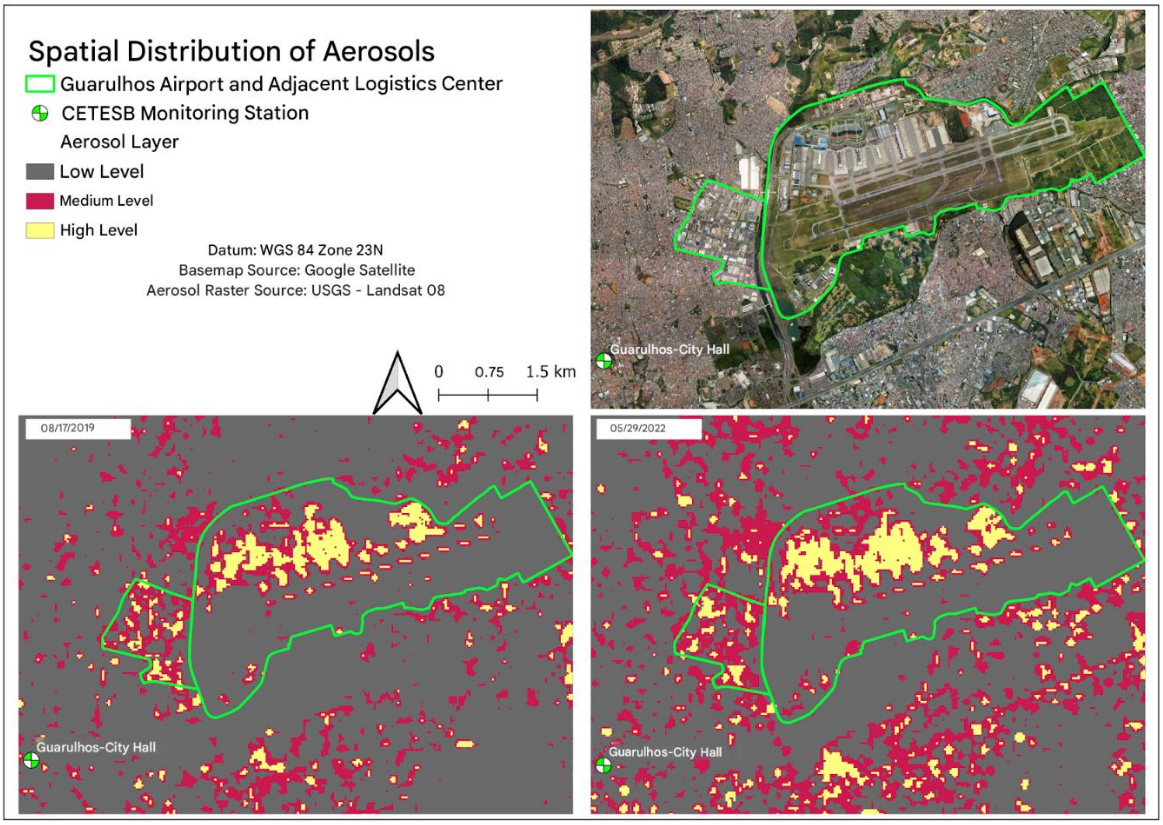

Figure 6. Guarulhos Airport in Guarulhos - SP.

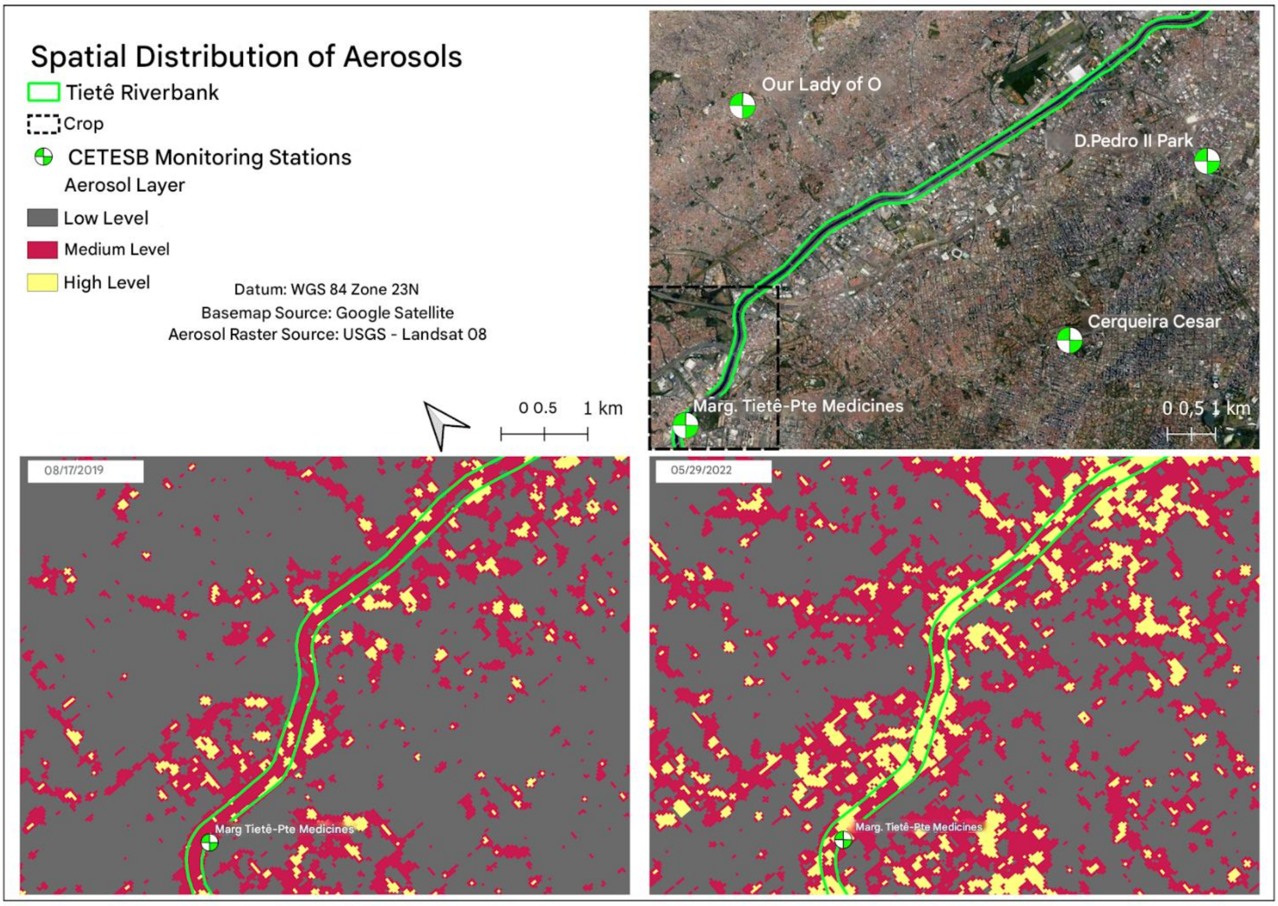

Figure 7. Margin of the Tietê River in São Paulo - SP.

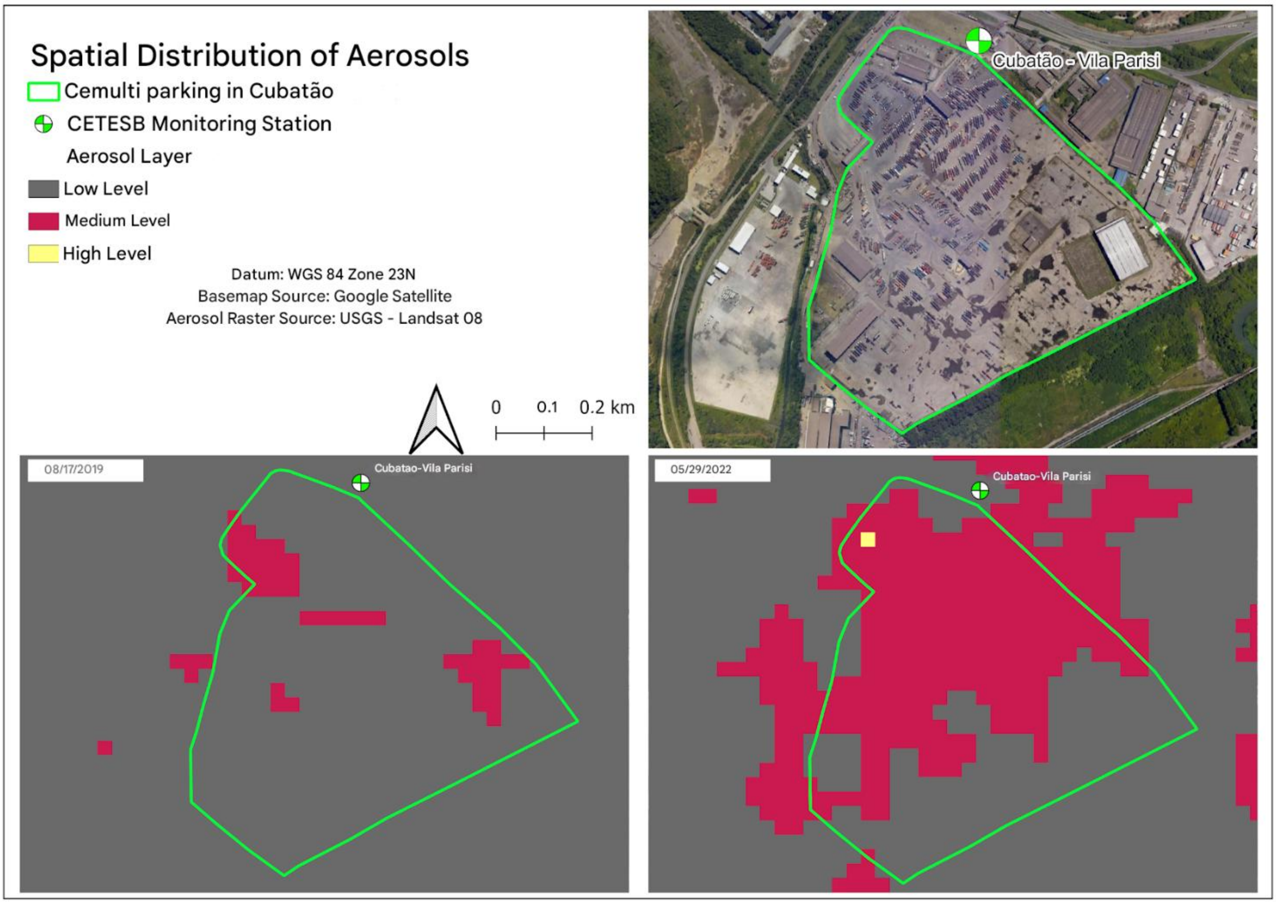

Figure 8. Cemulti parking lot in Cubatão - SP.

The analysis of the location of CETESB stations in areas with the highest vehicle traffic also raises questions about the measurement-scale mismatch between point-based monitoring stations and satellite-based mapping. For example, if the "Marginal Tietê - Ponte Remédios" monitoring station were relocated 60 meters northeast along Marginal Tietê (i.e., two Landsat pixels), it would be more centrally positioned within the aerosol concentration foci in both 2019 and 2022. The Cerqueira César station, despite being on a road with high vehicle flow, is also located in a heavily wooded segment, where trees may act as barriers and pollutant filters. Cubatão-Vale do Mogi station has high PM_{10} values and is located at the exit of the Terloc Cesari logistics warehouse garage, potentially capturing point emissions from vehicles leaving the facility, even though the surrounding area does not exhibit high regional aerosol levels in the satellite map. Cubatão-Vila Parisi (**Figure 8**) is located between two grassy areas with low mapped aerosol levels, but it lies on the connecting road between two logistics parking lots that are classified as high aerosol level, and thus may capture vehicle movement between the two parking lots, which is beyond the spatial resolution of Landsat imagery.

Mining areas

Figure **9** illustrates quarry areas, where there is intense movement of sand and other particulate materials. Due to the low density of these particles, on-site handling and transport (by vehicles or personnel) can emit particulate matter into the air. An increase in aerosol patches is observed in 2022. To mitigate aerosol impacts, measures are commonly recommended, such as dust suppression systems based on water spraying (humidification) and physical barriers (e.g., tree lines) to limit dispersion to surrounding areas (Saka et al., 2025). As in industrial warehouses, it is also worth noting that quarry surfaces can be highly reflective, potentially increasing uncertainty in aerosol estimation.

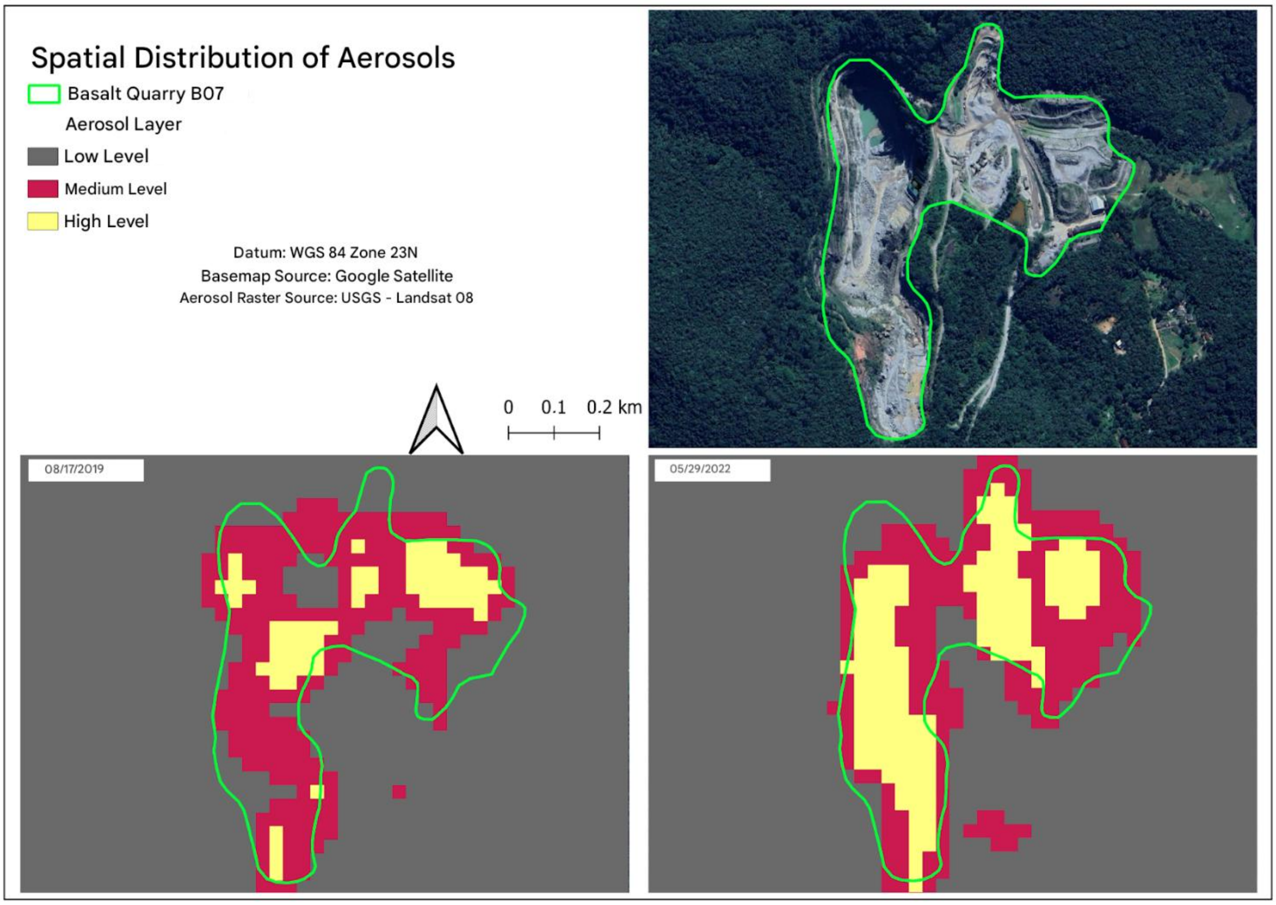

Figure 9. Quarry in Itapecerica da Serra - SP.

Other areas with water presence

Figures 10, **11,** and **12** were identified as areas with a high concentration of aerosol pixels, which may be mainly due to the presence of water.

Figure **10**, for example, corresponds to a large area of agricultural land with abundant, continuous irrigation. Although irrigation spraying is the most likely explanation for erroneous aerosol identification, other aerosol sources in agricultural areas cannot be ruled out, such as spraying of agrochemicals, crop/pasture burning, and aerosols of biological origin (e.g., pollen).

Figure **11**, on the other hand, represents areas with water bodies in Baixada Santista, including mangroves, rivers, and the sea. The sea may also contribute sea-salt aerosols, while beaches may contribute wind-blown sand and dust. Finally, Figure **12** represents extensive areas of high-end residential condominiums, where most buildings include swimming pools.

Notably, atmospheric water vapor and liquid water can introduce uncertainty into AOD retrievals (Vermote et al., 2016; Jin et al., 2022). Therefore, potential water-related interference should be considered and, where appropriate, excluded from aerosol-distribution analyses.

Figure 10. Agricultural area in Limeira - SP.

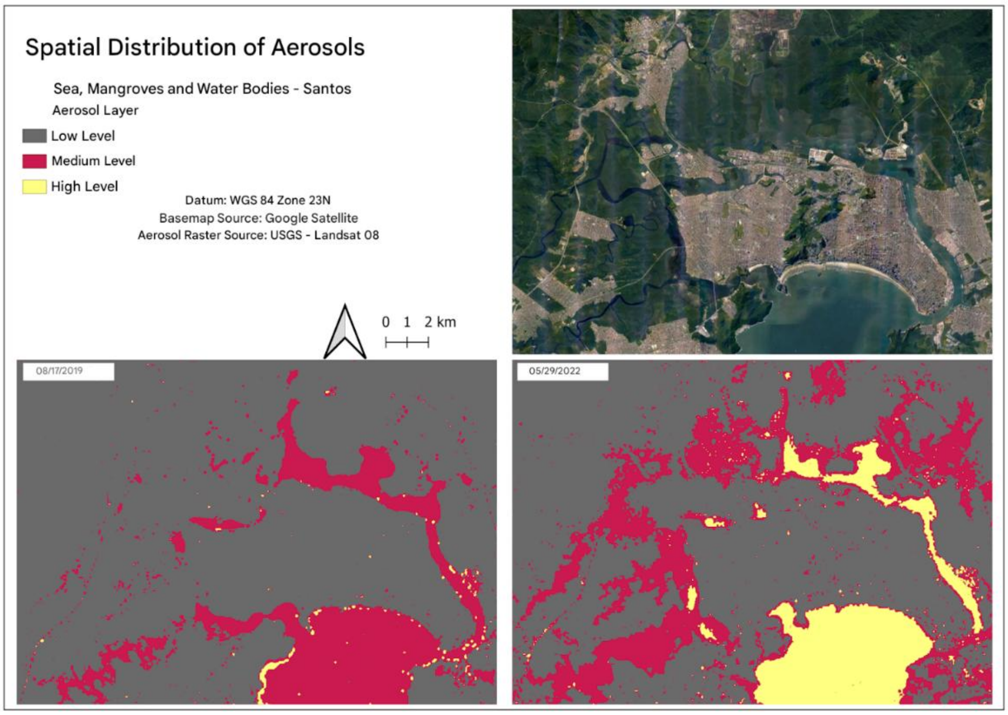

Figure 11. Water bodies (mangroves, rivers and sea) in Santos - SP.

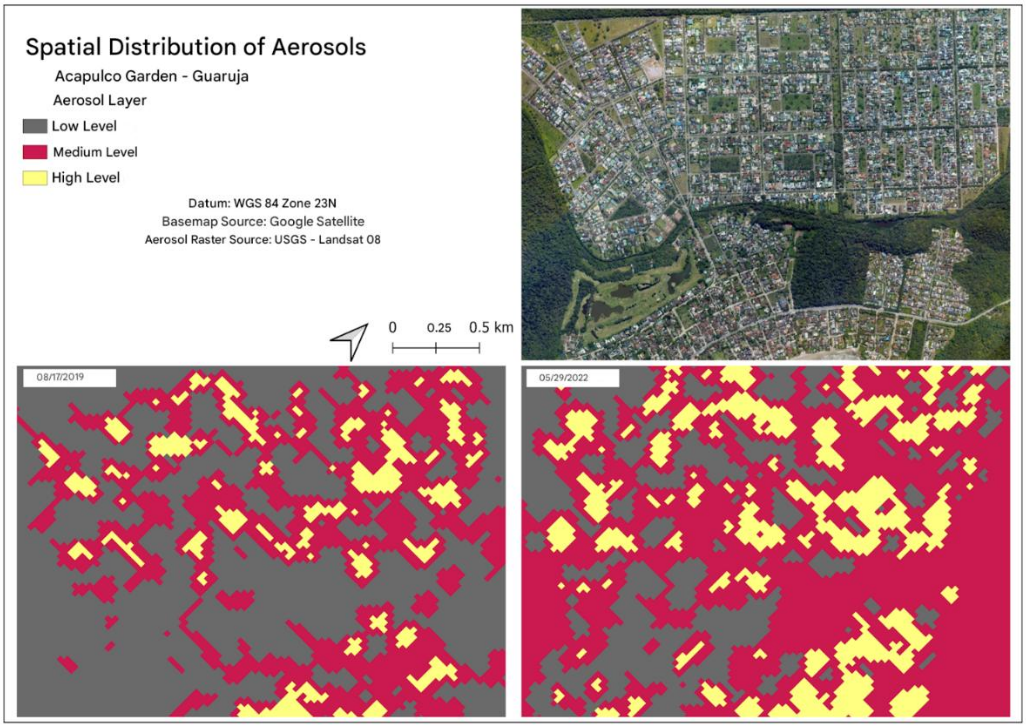

Figure 12. Jardim Acapulco neighborhood in Guarujá - SP. Source: The authors.

Conclusions

This study showed that high-resolution Landsat aerosol-level mapping is useful for tracking the dispersion of fine particulate matter and can support public health strategies aiming at reducing the adverse effects of urban air pollution. To critically assess fine-scale pollution dynamics across the highly industrialized Macrometropolitan Region of São Paulo and Baixada Santista, this study combined 30 m aerosol level data from Landsat 8 and 9 with ongoing ground-level monitoring data.

The main findings indicate that Landsat-derived AOD exhibits a strong capacity to detect localized spatial patterns of atmospheric aerosol dispersion that are not visible to conventional coarse-resolution global sensors. The satellite data effectively identified spatially coherent emission domains closely linked to major mining, industrial, and logistics zones, as well as dense corridors of heavy-duty transportation. Nevertheless, the relationship between point-based ground-level PM_{10} concentrations and total-column AOD retrievals appears complex and is strongly modulated by meteorological conditions. AOD signals may have been affected by hygroscopic aerosol growth under high relative humidity, while ground-level PM_{10} decreased, possibly due to concurrent wind-driven dispersion.

Landsat-based AOD data were the most suitable dataset for estimating near-surface urban atmospheric aerosols when compared to Sentinel-2 imagery. However, these data show inconsistencies in aerosol estimation over areas with large water surfaces, such as lakes, seas, and oceans, as well as irrigated agricultural areas. It is also important to note that the Landsat products were used only to retrieve AOD, since this study did not estimate PM concentrations separately; therefore, the aerosol signal also reflects particles formed through atmospheric processes, such as atmospheric vapor nucleation or gas condensation (Tuovinen et al., 2021).

Satellite-derived AOD products have inherent limitations due to cloud cover, which hinders continuous monitoring. Over the 10 years, only two cloud-free images covering the entire study area were suitable for aerosol mapping. Therefore, remote-sensing-based aerosol monitoring should be complementary to other measurement approaches.

Estimating AOD from Landsat sensors can improve monitoring station siting. Satellite imagery can provide an initial approximation of major particulate matter source areas, which can then be measured and validated in the field. This approach would allow stations to be positioned closer to the centers of key emission patches, and away from locations where local microclimates (e.g., heavily wooded segments) may interfere with dispersion patterns and measurements.

Most AOD retrieval methods perform better over dark surfaces, which can lead to poorer AOD estimates in urban, arid, and semiarid environments. Accordingly, conventional AOD retrieval approaches developed for low reflectance conditions may need to be adapted for bright surfaces, because aerosol signals are more difficult to isolate in high-reflectance pixels (Bilal et al., 2022). In such settings, it is advisable to combine satellite-based AOD products with complementary monitoring methods.

The aerosol patches identified in Landsat-8 imagery, especially in the Metropolitan Region of São Paulo, were consistent with emission sources identifiable in high-resolution satellite images. In the vicinity of the Metropolitan Region of Campinas, areas with the highest vehicle traffic were consistently mapped, but irrigated agricultural fields emerged as a potential source of uncertainty in attributing aerosol signals. In Baixada Santista, mapping coherence was impaired by high coastal humidity and water-rich covers (e.g., mangroves and swimming pools), as well as by potential contributions from sea-salt aerosols and coastal sediments.

In addition to monitoring, more restrictive environmental measures in industrial and logistics areas are advisable. To mitigate aerosol dispersion, vegetative barriers (windbreaks) can be used to separate emission sources from surrounding populations. In parallel, reducing the circulation of combustion-powered vehicles and/or increasing the use of electric vehicles in industrial and logistics facilities could reduce particulate emissions. Another priority is updating vehicle emission regulations to be more stringent, as current standards in Brazil are less strict than those in Europe and North America (Ribeiro et al., 2022).

This study provides a reproducible hotspot-screening workflow that complements ground station monitoring. It reveals fine-scale patterns and potential under-sampled areas when quality flags (e.g., water, bright surfaces, agricultural sources, and coastal influences) are explicitly addressed. Future work should extend the analysis to a longer time series. It should also incorporate meteorological variables and multi-sensor aerosol products to support quantitative concentration estimation, including uncertainty estimation and reporting.

Looking ahead, research should focus on advances in machine-learning and deep neural-network models to overcome the challenges posed by bright-surface conditions inherent in physically based radiative transfer models. By combining high-resolution satellite imagery with networks of affordable local sensors, cities could enable improved real-time calibration of pollution monitoring products. This fusion of data-driven models and ground-based observations can help translate column-integrated aerosol optical properties into more accurate, health-relevant surface $PM_{2.5}$ and PM_{10} mass metrics. Ultimately, this approach could support stronger, evidence-based urban environmental policies.

Acknowledgments

We thank Professors Claudia Boian and Nilton Manuel Évora do Rosário for helpful comments on preliminary versions of this article.

References

Abe, K. C., & Miraglia, S. G. E. K. (2016). Health impact assessment of air pollution in São Paulo, Brazil. *International Journal of Environmental Research and Public Health*, 13(7), 694. https://dx.doi.org/10.3390%2Fijerph13070694

Bilal, M., Mhawish, A., Ali, M. A., Nichol, J. E., Leeuw, G. D., Khedher, K. M., ... & Nazeer, M. (2022). Integration of surface reflectance and aerosol retrieval algorithms for multi-resolution aerosol optical depth retrievals over urban areas. *Remote Sensing*, *14*(2), 373. https://doi.org/10.3390/rs14020373

Bravo, M., Son, J., Freitas, C., Gouveia, N., & Bell, M. (2016). Air pollution and mortality in São Paulo, Brazil: Effects of multiple pollutants and analysis of susceptible populations. *Journal of Exposure Science and Environmental Epidemiology*, 26(2), 150-161. https://doi.org/10.1038/jes.2014.90

CETESB - Companhia Ambiental Do Estado De São Paulo, (2022). *Qualidade do ar no estado de São Paulo. São Paulo:* CETESB, 2022. https://cetesb.sp.gov.br/ar/wp-content/uploads/sites/28/2022/10/Relatorio-de-Qualidade-do-Ar-no-Estado-de-Sao-Paulo-2021.pdf

CETESB (2023). QUALAR - Sistema de informações da qualidade do ar. *Relatórios de Valores Diários*. https://qualar.cetesb.sp.gov.br

DataGeo - Sistema Ambiental Paulista, (2023). *Estações de Monitoramento*. São Paulo. https://datageo.ambiente.sp.gov.br/

Gavidia-Calderón, M., Schuch, D., Vara-Vela, A., Inoue, R., Freitas, E. D., Albuquerque, T. T. D. A., ... & Bell, M. L. (2024). Air quality modeling in the metropolitan area of São Paulo, Brazil: A review. *Atmospheric Environment*, *319*, 120301. https://doi.org/10.1016/j.atmosenv.2023.120301

Gouveia, N., Corrallo, F., Leon, A., Junger, W., & Freitas, C. (2017). Poluição do ar e hospitalizações na maior metrópole brasileira. *Revista de Saúde Pública*, 51, 117. https://doi.org/10.11606/s1518-8787.2017051000223

Groeneveld, D. P., Ruggles, T., & Gao, B. C. (2024). Landsat-8/9 Atmospheric Correction Reliability Using Scene Statistics. *Remote Sensing*, 16(12), 2216. https://doi.org/10.3390/rs16122216

Hamilton, D. S., Perron, M. M., Bond, T. C., Bowie, A. R., Buchholz, R. R., Guieu, C., ... & Mahowald, N. M. (2022). Earth, wind, fire, and pollution: Aerosol nutrient sources and impacts on ocean biogeochemistry. *Annual Review of Marine Science*, *14*(1), 303-330. https://doi.org/10.1146/annurev-marine-031921-013612

Han, L., Yan, H., Xiang, X., Liu, X., Shi, R., Wang, H., ... & Wang, H. (2021). Characteristics, evolution, and potential source regions of submicron aerosol in Beijing, China. *Atmospheric Environment*, *246*, 118061. https://doi.org/10.1016/j.atmosenv.2020.118061

Hoffmann, B., Boogaard, H., de Nazelle, A., Andersen, Z. J., Abramson, M., Brauer, M., ... & Thurston, G. (2021). WHO air quality guidelines 2021–aiming for healthier air for all: a joint statement by medical, public health, scientific societies and patient representative organisations. International journal of public health, 66, 1604465. https://doi.org/10.3389/ijph.2021.1604465

Jebali, A., Zare, M., Ekhtesasi, M. R., & Jafari, R. (2021). Detection of areas prone to wind erosion and air pollution using DSI and PDSI indices. *Natural Hazards*, *108*(1), 1221-1235. https://doi.org/10.1007/s11069-021-04728-3

Jin, Y., Hao, Z., Huang, H., Wang, T., Mao, Z., & Pan, D. (2022). Evaluation of LaSRC aerosol optical depth from Landsat-8 and Sentinel-2 in Guangdong-Hong Kong-Macao greater bay area, China. *Atmospheric Environment*, *280*, 119128. https://doi.org/10.1016/j.atmosenv.2022.119128

Leirião, L., de Oliveira, M., Martins, T., & Miraglia, S. (2023). A multi-pollutant and meteorological analysis of cardiorespiratory mortality among the elderly in São Paulo, Brazil—an artificial neural networks approach. *International Journal of Environmental Research and Public Health*, *20*(8), 5458. https://doi.org/10.3390/ijerph20085458

Li, J., Carlson, B. E., Yung, Y. L., Lv, D., Hansen, J., Penner, J. E., ... & Dong, Y. (2022). Scattering and absorbing aerosols in the climate system. Nature Reviews Earth & Environment, 3(6), 363-379. https://doi.org/10.1038/s43017-022-00296-7

Liu, Y., Huang, J., & Huang, F. (2023). A comprehensive review on study methods of aerosol optical properties in different dimensions. *IEEE Access*, *11*, 36763-36786. https://doi.org/10.1109/ACCESS.2023.3266333

Mansour, H. M., Muralidharan, P., & Hayes Jr, D. (2024). Inhaled nanoparticulate systems:

composition, manufacture and aerosol delivery. *Journal of Aerosol Medicine and Pulmonary Drug Delivery*, *37*(4), 202-218. https://doi.org/10.1089/jamp.2024.29117.mk

Meo, S. A., Salih, M. A., Alkhalifah, J. M., Alsomali, A. H., & Almushawah, A. A. (2024). Environmental pollutants particulate matter ($PM_{2.5}$, PM_{10}), Carbon Monoxide (CO), Nitrogen dioxide (NO2), Sulfur dioxide (SO2), and Ozone (O3) impact on lung functions. *Journal of King Saud University-Science*, *36*(7), 103280. https://doi.org/10.1016/j.jksus.2024.103280

NASA. AERONET: Aerosol Robotic Network — Aerosol Optical Depth (V3) data. Greenbelt: NASA Goddard Space Flight Center, 2023. Available at: https://aeronet.gsfc.nasa.gov/ . Accessed on: 14 Nov. 2023.

Nazeer, M., Ilori, C. O., Bilal, M., Nichol, J. E., Wu, W., Qiu, Z., & Gayene, B. K. (2021). Evaluation of atmospheric correction methods for low to high resolutions satellite remote sensing data. *Atmospheric Research*, *249*, 105308. https://doi.org/10.1016/j.atmosres.2020.105308

Pérez-Martínez, P. J., Magalhaes, T., Maciel, I., de Miranda, R. M., & Kumar, P. (2022). Effects of the COVID-19 pandemic on the air quality of the metropolitan region of Sao Paulo: analysis based on satellite data, monitoring stations and records of annual average daily traffic volumes on the main access roads to the city. Atmosphere, 13(1), 52. https://doi.org/10.3390/atmos13010052

Putman, W. (2014). *GEOS-5 Aerosols Simulation for SC* NASA's Goddard Space Flight Center/Global Modeling and Assimilation Office. https://svs.gsfc.nasa.gov/3063

Qayyum, F., Tariq, S., Ul-Haq, Z., Mehmood, U., & Zeydan, Ö. (2022). Air pollution trends measured from MODIS and TROPOMI: AOD and CO over Pakistan. *Journal of Atmospheric Chemistry*, *79*(3), 199-217. https://doi.org/10.1007/s10874-022-09436-1

Qi, L., Liu, R., & Liu, Y. (2022). Retrieval of aerosol single-scattering albedo from MODIS data using an artificial neural network. Remote Sensing, 14(24), 6341. https://doi.org/10.3390/rs14246341

Qin, X., Do, T. H., Hofman, J., Bonet, E. R., La Manna, V. P., Deligiannis, N., & Philips, W. (2022). Fine-grained urban air quality mapping from sparse mobile air pollution measurements and dense traffic density. *Remote Sensing*, *14*(11), 2613. https://doi.org/10.3390/rs14112613

Ranjan, A. K., Patra, A. K., & Gorai, A. K. (2021). A review on estimation of particulate matter from satellite-based aerosol optical depth: Data, methods, and challenges. *Asia-Pacific Journal of Atmospheric Sciences*, *57*, 679-699. https://doi.org/10.1007/s13143-020-00215-0

Ribeiro, C. B., Rodella, F. H. C., & Hoinaski, L. (2022). Regulating light-duty vehicle emissions: an overview of US, EU, China and Brazil programs and its effect on air quality. *Clean Technologies and Environmental Policy*, *24*(3), 851-862. https://doi.org/10.1007/s10098-021-02238-1

Rodriguez-Loya, J., Lerma, M., & Gardea-Torresdey, J. L. (2023). Dynamic light scattering and its application to control nanoparticle aggregation in colloidal systems: a review. Micromachines, 15(1), 24. https://doi.org/10.3390/mi15010024

Rudke, A. P., Martins, J. A., Hallak, R., Martins, L. D., De Almeida, D. S., Beal, A., ... & Albuquerque, T. T. A. (2023). Evaluating TROPOMI and MODIS performance to capture the dynamic of air pollution in São Paulo state: A case study during the COVID-19 outbreak. *Remote sensing of environment*, *289*, 113514. https://doi.org/10.1016/j.rse.2023.113514

Saka, M. B., Mohd Hashim, M. H., & Shehu, S. A. (2025). Mining dust: health impacts, control measures and future directions. *Environmental Engineering & Management Journal (EEMJ)*, 24(2). https://doi.org/10.30638/eemj.2025.032

Shah, M., Raval, M. S., & Divakaran, S. (2025). A systematic review on deep learning for atmospheric correction of satellite images. *Archives of Computational Methods in Engineering*, 1-31. https://doi.org/10.1007/s11831-025-10424-3

Sheng, Q., Ji, Y., Zhou, C., Zhang, H., & Zhu, Z. (2023). Spatiotemporal variation and pattern analysis of air pollution and its correlation with NDVI in Nanjing City, China: A Landsat-Based study. *Forests*, *14*(10), 2106. https://doi.org/10.3390/f14102106

Singer, J. M., André, C. D. S., André, P. A., Rocha, F. M. M., Waked, D., Vaz, A. M., ... & Barrozo, L. V. (2023). Assessing socioeconomic bias of exposure to urban air pollution: an autopsy-based study in São Paulo, Brazil. *The Lancet Regional Health–Americas*, *22*. https://doi.org/10.1016/j.lana.2023.100500

Soleimany, A., Solgi, E., Ashrafi, K., Jafari, R., & Grubliauskas, R. (2022). Temporal and spatial distribution mapping of particulate matter in southwest of Iran using remote sensing, GIS, and statistical techniques. *Air Quality, Atmosphere & Health*, *15*(6), 1057-1078. https://doi.org/10.1007/s11869-022-01179-y

Sun L., Wei J., Bilal M., Tian X., Jia C., Guo Y., & Mi X. (2016). Aerosol Optical Depth Retrieval over Bright Areas Using Landsat 8 OLI Images. Remote Sensing. 8(1), 23. https://doi.org/10.3390/rs8010023

Tang, X., & Kumar, R. (2022). Promoting the Implementation of the Ambitious 2021 WHO Global Air Quality Guidelines in Asia. *Bulletin of the American Meteorological Society*, 103(7), E1684-E1690. https://doi.org/10.1175/BAMS-D-22-0040.1

Tuovinen, S., Kontkanen, J., Cai, R., & Kulmala, M. (2021). Condensation sink of atmospheric vapors: the effect of vapor properties and the resulting uncertainties. *Environmental Science: Atmospheres*, *1*(7), 543-557. https://doi.org/10.1039/D1EA00032B

USGS - United States Geological Survey. (2020). *Landsat 8 Collection 1 (C1) Land Surface Reflectance Code (LaSRC) - Product Guide*. https://d9-wret.s3.us-west-2.amazonaws.com/assets/palladium/production/s3fs-public/atoms/files/LSDS-1368_L8_C1-LandSurfaceReflectanceCode-LASRC_ProductGuide-v3.pdf

USGS - United States Geological Survey. (2023). EarthExplorer. United States of America. https://earthexplorer.usgs.gov/

Vermote, E., Justice, C., Claverie, M., & Franch, B. (2016). Preliminary analysis of the performance of the Landsat 8/OLI land surface reflectance product. *Remote sensing of environment*, *185*, 46-56. https://doi.org/10.1016/j.rse.2016.04.008

WHO World Health Organization. (2023). World health statistics 2023: monitoring health for the SDGs sustainable development goals. https://www.who.int/publications/i/item/9789240074323

Wikuats, C. F. H., Nogueira, T., Squizzato, R., de Freitas, E. D., & Andrade, M. D. F. (2023). Health risk assessment of exposure to air pollutants exceeding the new WHO air quality guidelines (AQGs) in São Paulo, Brazil. *International Journal of Environmental Research and Public Health*, *20*(9), 5707. https://doi.org/10.3390/ijerph20095707

Xu, P. W., Tan, X. P., Cai, J. Z. & Liu, J. S. (2005). Study on Influence Factors of Urban Aerosol on Visibility and Extinction Coefficient. *Environ. Pollut. Control*, 27, 410–413.

Zhu, H., Martin, R. V., Van Donkelaar, A., Hammer, M. S., Li, C., Meng, J., ... & Lyapustin, A. (2024). Importance of aerosol composition and aerosol vertical profiles in global spatial variation in the relationship between PM 2.5 and aerosol optical depth. *Atmospheric Chemistry and Physics*, *24*(20), 11565-11584. https://doi.org/10.5194/acp-24-11565-2024